Resolution and speed improvements of mid infrared Fabry-Perot microspectrometers for the analysis of hydrocarbon gases

Martin Ebermann*[1], Norbert Neumann[1], Karla Hiller[2], Mario Seifert[2], Marco Meinig[3], Steffen Kurth[3]

[1] InfraTec GmbH, Gostritzer Str. 61–63, 01217 Dresden, Germany

[2] Universität Chemnitz, Zentrum für Mikrotechnologien, 09107 Chemnitz, Germany

[3] Fraunhofer ENAS, Technologie-Campus 3, 09126 Chemnitz, Germany

ABSTRACT

Micromachined tunable Fabry-Pérot filters (µFPF) are key elements in a new class of miniature spectrometers and analyzers. Different groups all over the world are working on µFPF for spectral ranges from the visible up to the long wave infrared. In order to achieve a large tuning range, the filters are normally operated in the first interference order. At the same time the spectral resolution is limited due to a limited effective finesse. A variety of applications demand for higher resolutions. This is particularly true for the multicomponent analysis of hydrocarbon gases, because the individual absorption bands are very similar and widely overlapping. In this paper µFPF in 3rd and 4th order configuration with a spectral resolution of about (20...30) nm and a tuning range of (3.1...3.7) µm are presented. For the measurement of additional gases in adjacent ranges (e.g. CO_2 around 4.3 µm) a dualband configuration with simultaneous use of different orders is proposed. A largely reduced damping of the µFPF and the combination with a lead selenide photoresistor instead of a thermal detector allows for a fast acquisition of spectra.

1. INTRODUCTION

The measurement of hydrocarbon gases with high accuracy and the discrimination of components in mixtures is strongly desired in many applications. This is especially true in the analysis of natural gas, biogas or other fuel gases to determine their energy content for billing purposes or to control combustion processes. Nowadays, for such sensing tasks the gas chromatograph (GC) is the "Gold-Standard". But it has several disadvantages: Beside its high costs it requieres carrier gas, usually helium. Furthermore the analysis with a GC is quite slow, a measurement takes up to several minutes.

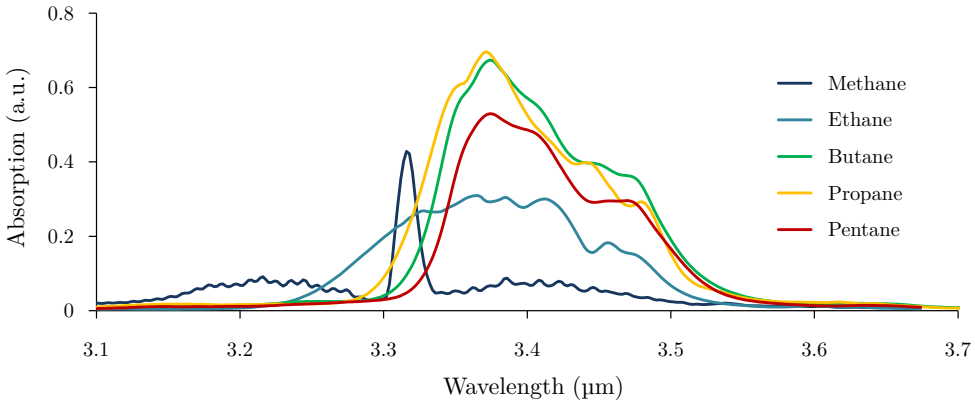

Figure 1. Absorption spectra of the C1 - C5 alkanes (qualitative representation, data taken from NIST[1]).

* m.ebermann@infratec.de; phone +49 351 871 8625; fax +49 351 871 8727; www.infratec.de

A potentially faster and much cheaper solution is the use of infrared absorption spectroscopy, which is a widely used method in gas analysis. Figure 1 is a qualitative representation of the absorption spectra of the C1 - C5 alkanes, which are the main components of interest in the analysis of fuel gases. In most cases carbon dioxid should also be measured for reliable results.

A classical IR gas analyzer is comprised of an IR emitter, a gas cell and one or more detector channels which are equipped with narrowband optical filters. The filter wavelengths (center wavelength, *CWL*) are adjusted to the specific absorption bands of the target gases. The filter bandwidth (full width at half maximum, *FWHM*) is normally in the order of $1 \ldots 5$ % of the wavelength. Such systems are already used for the analysis of natural gas. Three channels are required at least: one for the integral absorption of the hydrocarbon components, centered around 3.4 µm, one for carbon dioxid around 4.3 µm and one reference channel at a wavelength free of absorption to compensate for drifts.[2] Such simple systems function properly for more or less "normal" mixtures because the measured integral hydrocarbon absorbance is nearly proportional to the energy content of the gas, but they come to their limit in case of more complexe mixtures.

The solution proposed in this paper is to use a microspectrometer instead of fixed filters. For this purpose tunable filters are especially suited since they provide a throughput advantage over grating spectrometers or linear variable filters with detector arrays. FOURIER-transform spectrometers with their multiplex advantage on the other hand are much more complex devices.

The key issues for this kind of applications are the optimum wavelength range and the needed spectral resolution. The range $(3.1 \ldots 3.7)$ µm is clearly preferred over shorter wavelengths, because the gas components (except CO_2) are quite strong absorbing in this range. The issue of the best resolution is much more difficult to tackle, because the absorption spectra of the alkanes are in general very similar. A very high resolution of only a few nanometers might be desirable but this would seriously limit the optical throughput. A filter bandwidth in the range of $(20 \ldots 30)$ nm seems to be a reasonable compromise to achieve a significant progress compared to the state of the art. Apart from the problem of a full discrimination of all components this resolution will surely provide more spectral information and therefore a significant benefit for the measurements.

A spectrometer with rotating narrowband filters has already been succesfully applied.[3,4] The exact filter bandwidths have not been reported in the literature, but it can be assumed, that it is in the range proposed above. Our approach is the use of a tunable MEMS FABRY-PÉROT filter, which is potentially a more compact and cost effective solution. To increase the spectral resolution compared to earlier developments[5] it is now operated in higher interference orders. The throughput losses due to the higher resolution should be compensated by the use of a fast PbSe detector. A very similar approach was developed at VTT (Finland).[6] In contrast to the work described here, a µFPF in the 1st order is used, which limits the resolution to about 50 nm.

2. MICROMECHANICAL FABRY-PÉROT FILTERS

2.1 Optical considerations

The FABRY-PÉROT interferometer (FPI) is comprised of two parallel reflectors, normally embedded in air, arranged at the distance d_{opt} forming an optical half resonator (cavity). Its spectral transmittanc is described by the AIRY-formula[7]

$$T_{\mathrm{FPI}} = \frac{T^2}{(1-R)^2}\left[1 + F\sin^2\left(\frac{2\,\pi\, d_{\mathrm{opt}}\cos\theta}{\lambda}\right)\right]^{-1} \quad , \tag{1}$$

where R and T are the reflectance and the transmittance of the two reflectors, θ is the incidence angle. F is known as the finesse coefficient

$$F = \frac{4R}{(1-R)^2} \ , \tag{2}$$

and $\widetilde{F}$ as the Finesse

$$\widetilde{F} = \frac{\pi\sqrt{F}}{2} = \frac{\pi\sqrt{R}}{(1-R)} \quad , \tag{3}$$

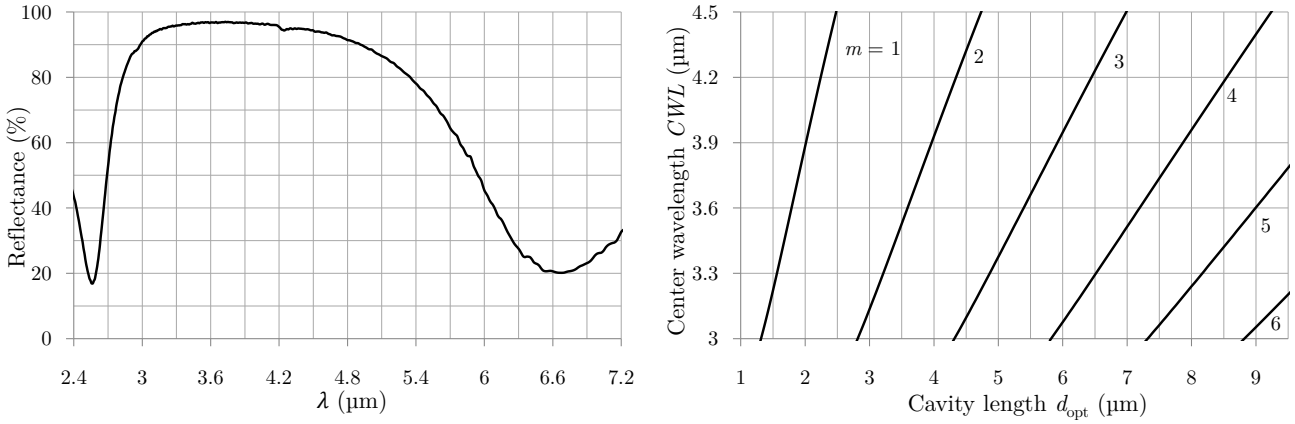

a) b)

Figure 2. $|HL|^2$ BRAGG-reflector ($\lambda_{\mathrm{ref}} = 3.6\,\mu\mathrm{m}$) made from polysilicon (n_H=3.4) and SiO_2 (n_L=1.33); a) Measured spectral reflectance, b) calculated optical transfer function $CWL\,(d_{\mathrm{opt}})$ of an µFPF with this reflector for the interference orders $m = 1 \ldots 5$.

or more precisely also referred to as reflectivity finesse $\widetilde{F}_R$. Reflectance phase dispersion is neglected for simplicity. The FPI transmittance consists of a series of transmission peaks (with order numbers m) at wavelengths CWL for which the resonance condition

$$CWL = \frac{2\,d_{\mathrm{opt}}}{m} \tag{4}$$

is fulfilled. The separation distance of successive orders is called free spectral range *FSR*. It also depends on m in the wavelength domain:

$$FSR_\lambda = \frac{2\,d_{\mathrm{opt}}}{m\,(m+1)} \quad . \tag{5}$$

Figure 2 shows the stopp-band of the BRAGG-reflector used in this work and the optical transfer function $CWL\,(d_{\mathrm{opt}})$ for the interference orders $m = 1 \ldots 5$. The 1st order ($m = 1$) provides the largest possible tuning range, normally limited by the width of the stopp-band of the used reflector. For higher orders the *FSR* becomes the limiting factor. The higher the order the lower is the tuning range.

The *FWHM* bandwidth is ideally given by

$$FWHM_\lambda = \frac{4\,d_{\mathrm{opt}}}{\pi\,m^2\sqrt{F}} \quad . \tag{6}$$

The spectral resolving power can be approximately calculated with

$$\mathcal{R} = \frac{CWL}{FWHM_\lambda} \approx m\,\widetilde{F} \quad . \tag{7}$$

Eq. 7 indicates, that there are two possible ways to increase the resolution, by increasing the finesse and by chosing a higher order. Unfortunately the first option is practically limited by the presence of defects (imperfections of the parallel reflector alignment and flatness) and the effect of a limited aperture (cone angle of the transmitted beam).[7] Both effects contribute to the so called effective finesse $\widetilde{F}_E$ which is a figure of the overall performance of the real FPI:

$$\frac{1}{\widetilde{F}_{\mathrm{E}}^2} = \frac{1}{\widetilde{F}_{\mathrm{R}}^2} + \frac{1}{\widetilde{F}_{\mathrm{D}}^2} + \frac{1}{\widetilde{F}_{\mathrm{A}}^2}\,, \tag{8}$$

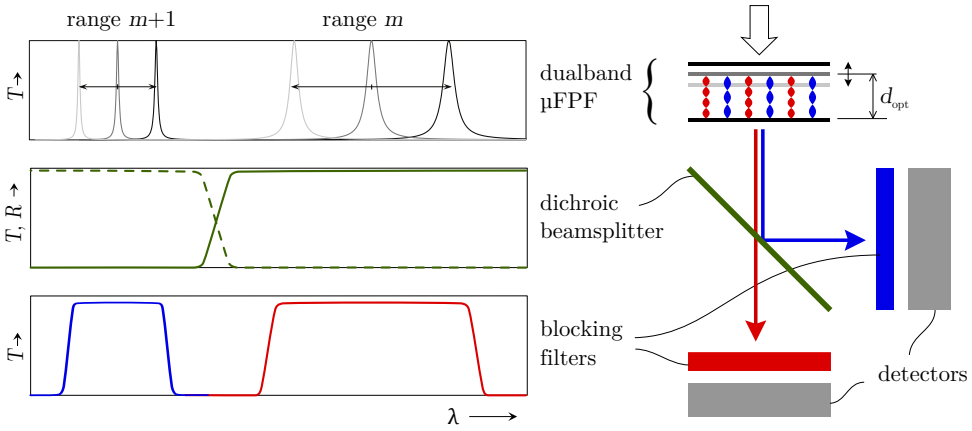

Figure 3. Schematic view and optical filtering scheme of a dual-channel spectrometer module with a dualband µFPF.

which means, that even if $\widetilde{F}_R$ is very high, $\widetilde{F}_E$ can never exceed $\widetilde{F}_D$ or $\widetilde{F}_A$. Practically achievable figures for µFPF with a sufficiently large aperture of a few millimeters are in the range of $\widetilde{F}_E = 40 \ldots 65$. For $m = 1$ this translates into $\mathcal{R} = 40 \ldots 65$ or $FWHM_\lambda = (50 \ldots 80)$ nm for the targeted wavelength range. A filter bandwidth of $(20 \ldots 30)$ nm which we aim for in this work corresponds to $\mathcal{R} \approx 150$ and therefore m should be ≥ 3.

As shown above (2) increasing the order is limited by the desired tuning range. Another reason not to push the order too high is the above mentioned aperture finesse $\widetilde{F}_A$. It is inversely proportional to m and it depends on the (full) cone angle α, which has a decisive influence on the optical througput of the filter:

$$\widetilde{F}_\mathrm{A} = \frac{8}{m\alpha^2} \,. \tag{9}$$

Therefore, increasing the order also means decreasing the cone angle if $\widetilde{F}_E$ should be maintained. In any case, tuning range, spectral resolution and throughput has to be carefully balanced. In this work we finally decided to use the 3rd or 4th order, which restricts the cone angle to about $\alpha = 5° \ldots 10°$.

2.2 Dual-band configurations

For the measurement of hydrocarbon gases, a tuning range $(3.1 \ldots 3.7)$ µm is sufficient. However, some applications require the additional measurement of CO_2 at its strong absorption band around 4.3 µm. We aim for tuning range of $(4.0 \ldots 4.6)$ µm here. As described above, an overall tuning range of $(3.1 \ldots 4.6)$ µm in one single interference and a high spectral resolution are not possible at the same time. The only way out is to use two consecutive orders simultaneously and to separate them by additional filtering (figure 3). The autors have already presented this concept of a dualband µFPF for the measurement of anesthesia gases and CO_2 in the spectral ranges $(4 \ldots 5)$ µm and $(8 \ldots 11)$ µm.[8] For this specific application a reflector with two stopp-bands (dualband reflector) was designed, whereas the bandwidth of a classical BRAGG reflector is sufficient for the range needed here (figure 2). The combination of the 3rd and 4th order is particularly suitable for this task, because the ranges $(3.1 \ldots 3.7)$ µm and $(4.0 \ldots 4.6)$ µm are covered exactly in parallel within these two orders with the same optical cavity length.

2.3 MEMS design

The basis for the work described here is the previous development of 1st order µFPF.[5] The filters are realized in bulk MEMS technology. They consist of two structured wafers, the first carrying the fixed reflector and driving electrodes, the second is equipped with springs and supports the movable reflector. Both wafers are bonded together by an intermediate SU-8 layer, which defines the initial plate separation (figure 4a). The aperture diameter of the filter is about 2 mm, the chip size is (8.5×8.5) mm^2. The filters are electrostatically actuated with tuning voltages of about 35 V.

As one of the advantages of the described structure the separation of the driving electrodes can be designed independently from the optical cavity length d_opt. By this way, one can avoid the electrostatic pull-in effect,

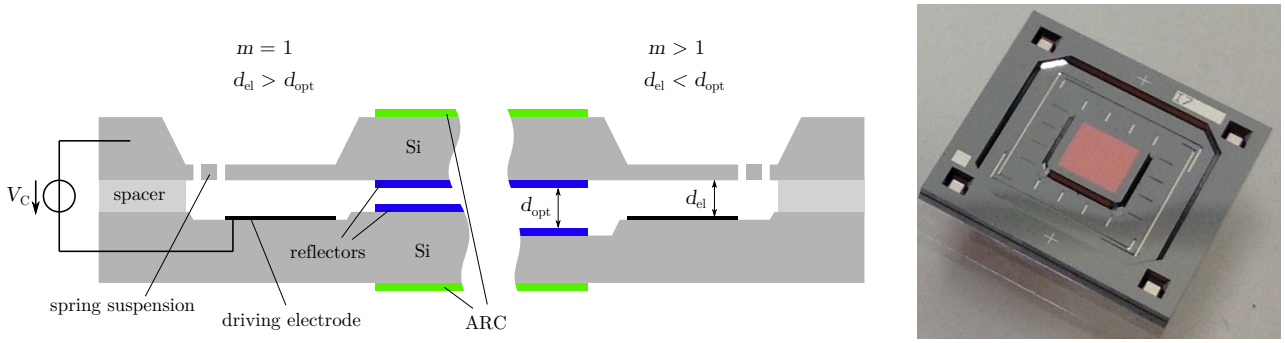

a) b)

Figure 4. µFPF fabricated with bulk MEMS technology; a) Schematic cross section of electrostatically actuated , left: 1st order configuration, right: higher order configuration; b) photograph of a fabrictated prototype.

which limits the stable mechanical tuning range to one third of the initial electrode distance d_{el}. Therefore, in the 1st order configuration d_{el} has to be larger than d_{opt}. In the 3rd or 4th order this relation should be inverse because the mechanical displacement to tune over one *FSR* remains constant. Otherwise a much higher control voltage would be required.

Modeling, simulation and measurement results of the electromechanical system of such filters has been discussed in detail in previous papers.[9,10] Here we only want to stick at the fact that the dynamic behavior is dominated by squeeze film damping. The mechanical time constants of previously realized 1st order filters are in the range of (12 . . . 60) ms. In order to reduce squeeze film damping vent holes in the electrode area were introduced for the new prototypes. In higher orders the damping is automatically reduced by a larger optical cavity. Additionally, smaller electrode areas (figure 4b) were used here. Furthermore, the spring stiffness could be increased, but this would be at the expense of higher control voltages.

2.4 Characterization

Prototypes of filters with 2nd & 3rd order configuration and with 3rd & 4th order configuration have been fabricated and tested. For a better comparison, 1st order filters were also made, which are nearly identical to the previous design, with exception of the venting holes.

Measurements of the spectral transmittance were carried out with an FTIR spectrometer (Bruker Vertex 70) with an resolution of 4 cm^{-1}. In case of the higher order filters the cone angle of the illuminating beam was reduced to about 6° by means of an circular iris diapraghm in the parallel beam behind the interferometer of the FTIR spectrometer. For the 1st order filters the full cone angle of the spectrometer of about 13° was applied.

The resulting spectra of three filters are shown in figure 5. The 1st order µFPF provides a large FSR of about 1.8 µm. This enables to tune over the full range of (4.0 . . . 4.6) µm, but the resolution is limited to about (50 . . . 80) nm.

The *FSR* of 840 nm of the 2nd & 3rd order filter allows for a slightly larger tuning range than (3.1 . . . 3.7) µm. The *FWHM* ranges from 23 nm to 30 nm. The upper region for the CO_2 measurement is not fully covered because the configuration would require a large mechanical displacement of about $\Delta d \approx 1.7\,\mu\mathrm{m}$, for which the MEMS system was not yet optimized. The filter with 3rd & 4th order configuration could be tuned over (3.1 . . . 3.65) µm, but the *FSR* of 645 nm would also allow for a slightly larger range to meet the requirements. Here, the *FWHM* ranges from 17 nm to 21 nm. The upper region (4.0 . . . 4.6) µm is fully covered within the 3rd order for which a mechanical deflection of about $\Delta d \approx 1.3\,\mu\mathrm{m}$ is needed. In all of the three cases a high peak transmittance of >60 % was demonstrated.

Measurements of the dynamic behavior were performed with the so called Step-Scan FTIR method,[11] for which an mercury cadmium telluride detector (MCT, cooled with liquid nitrogen) was used. The filters were excited with small voltage steps around several operating points (DC offset voltage) over the full tuning range. The results (figure 6) showed that the time constants significantly dependend on the mirror deflection or the control voltage respectively. This well known behavior is due to the electrostatic softening effect under voltage control,

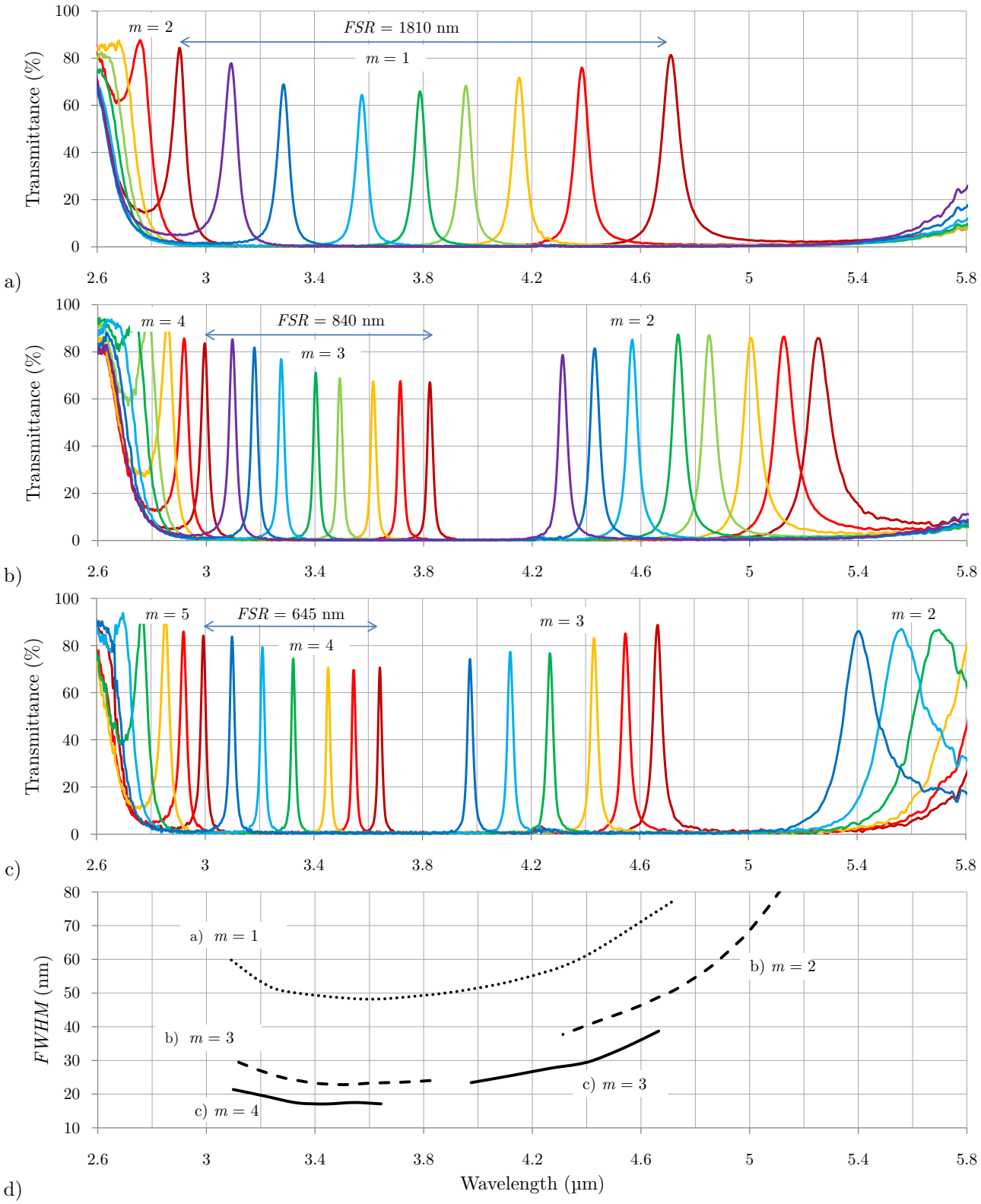

Figure 5. Spectral transmittance of µFPF prototypes at different tuning voltages, a) filter in 1st order configuration, b) 2nd & 3rd order configuration, b) 3rd & 4th order configuration, c) spectral resolution (*FWHM*) of the three configurations a) – c) (measured with FTIR spectrometer Bruker Vertex 70, resolution 4 cm^{-1}, full cone angle a) 13°, b) and c) 6°).

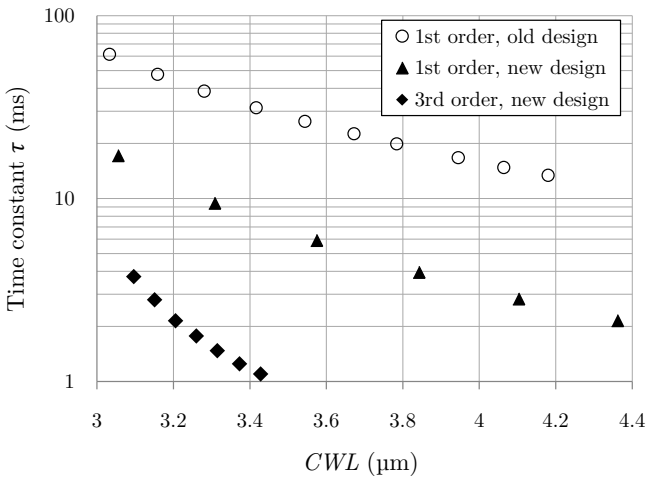

Figure 6. Mechanical time constant τ of a fabricated µFPF in 3rd order configuration as function of the filter wavelength CWL (Step-Scan measurement with FTIR spectrometer Bruker Vertex 70, N_2-cooled MCT detector).

through which the overall stiffness of the actuator is reduced with increasing deflection.[10] The introduction of the vent holes reduces the damping by a factor of five, whereas all other parameters, which have an impact on the time constant (spring stiffness, plate areas) are nearly identical compared to the old design. The 3rd filter has smaller electrodes. The spring stiffness was slightly reduced to maintain the voltage requirement to about $(35 \ldots 40)$ V. For this type, time constants of $\tau = (0.7 \ldots 4)$ ms were measured, which is a large further improvement. It allows for a scan frequency of 10 Hz at least.

3. INTEGRATED DETECTOR MODULE

The µFPF are integrated in a TO8 housing together with a IR detector. In previous developments[5] pyroelectric detectors with a specific detectivity of $D^* \approx 6 \times 10^8\,\mathrm{cm}\,\sqrt{\mathrm{Hz}}/\mathrm{W}$ ($T_{\mathrm{bb}} = 500\,\mathrm{K}$, $f = 10\,\mathrm{Hz}$, $\triangle f = 1\,\mathrm{Hz}$) were used. Pyroeletric detectors are very temperature stable and can be operated at room temperature. On the other hand they need a chopped or pulsed IR source and are limited to low modulation frequencies. Therefore, the aquisition of a complete spectrum has to be done stepwise and takes a few seconds.

Photon detectors have the advantage of a much higher detectivity over a wide frequency range. On the other hand their spectral response is limited to a certain wavelength range and additionally it is very temperature dependend.[12] Nevertheless, the high detectivity and the suitability for high modulation frequencies make them

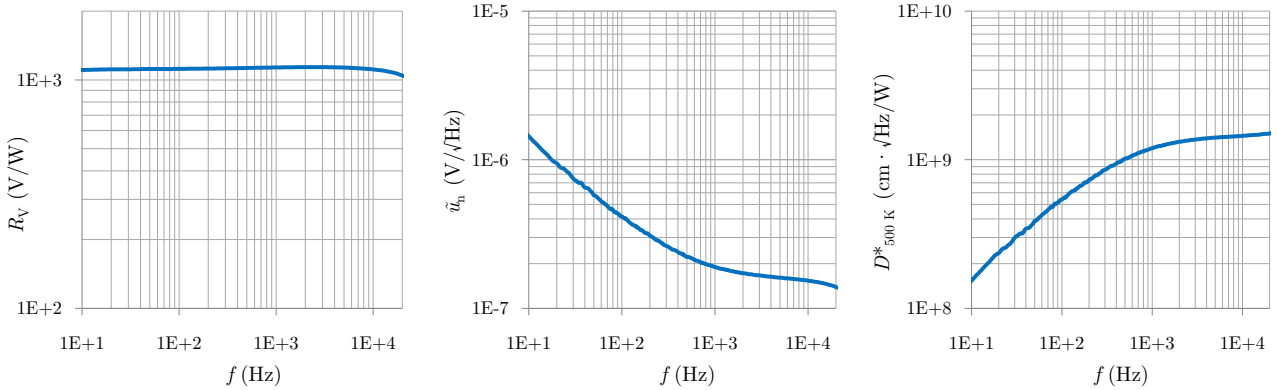

Figure 7. Frequency response of a typical PbSe photoresistor with (2×2) mm^2 element size: a) blackbody responsivity, b) noise density spectrum, c) specific detectivity ($T_{\mathrm{bb}} = 500\,\mathrm{K}$, $\triangle f = 1\,\mathrm{Hz}$, $R_{\mathrm{L}} = 1\,\mathrm{M\Omega}$ $V_{\mathrm{bias}} = 50\,\mathrm{V}$, $T = 23°\mathrm{C}$).

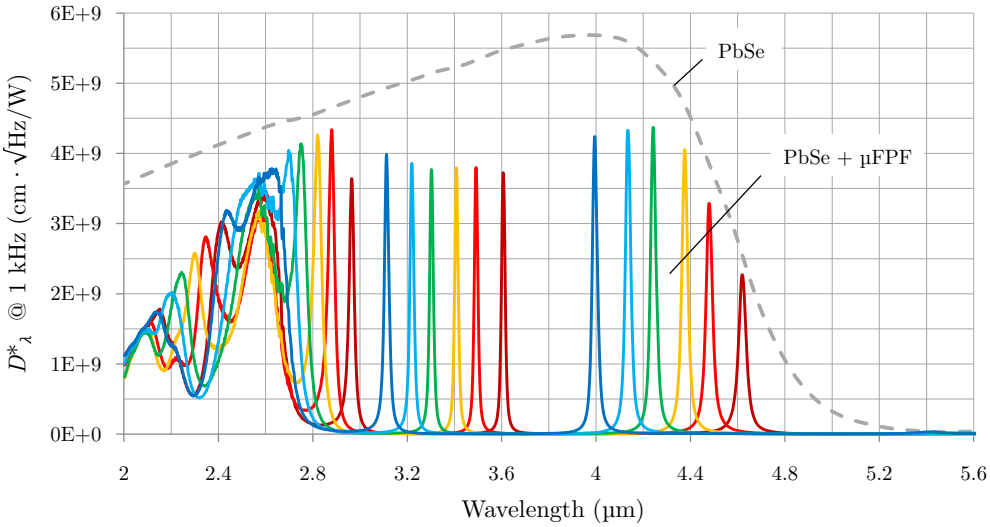

Figure 8. Spectral response (specific spectral detectivity) of a typical PbSe photoresistor (dashed curve) and an integrated microspectrometer module with the latter and a µFPF in 3rd & 4th order configuration (solid curves) without additional blocking filters.

the first choice for fast and high resolving microspectrometers. Since they can be also DC operated source modulation is not absolutely necessary. This enables an alternative very fast scanning method, in which the filter is continuously tuned and the measured spectrum is directly represented by the detector output in the time domain.

In this work lead selenide (PbSe) photoresistors are used, because their spectral response spans over a range up to 4.8 µm at room temperature. They are further characterized by a dark resistance of (0.2 . . . 2) MΩ and they need a bias voltage of about 50 V to 100 V. Electro-optical characterization of different types from several manufacturers were performed. Figure 7 shows typical results.

For spectral measurements a pyroelectric detector with a silver black coating has served as reference, because it has a very flat spectral response. Measurements with the blackbody source and a narrow band pass filter centered at 3.95 µm revealed that the peak response is about 5 times higher than the blackbody response (500 K). Spectra were again aquired with an FTIR spectrometer. Figure 8 shows the specific spectral detectivity of a bare PbSe element as well as that of an integrated detector module with a µFPF mounted on top.

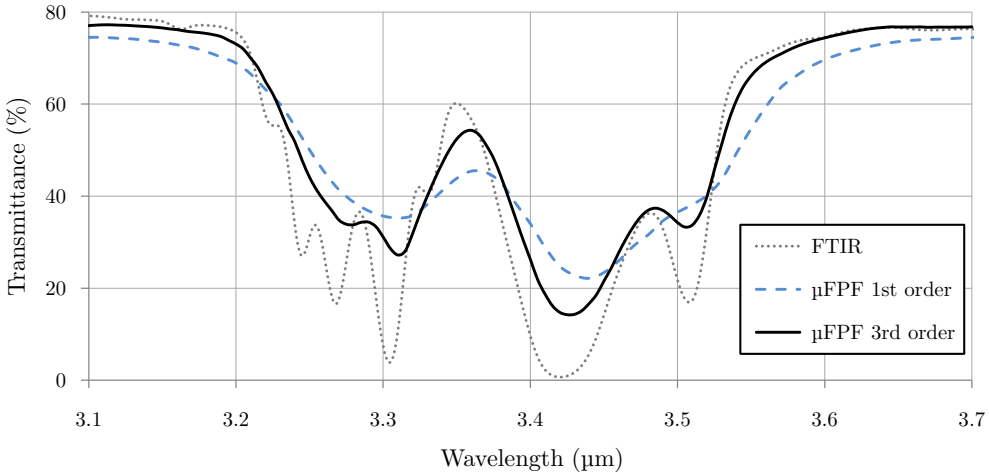

Figure 9. Transmittance spectra of a 0.4 mm thick polystyrene foil measured with a FTIR spectrometer (dotted curve, resolution 8 cm^{-1}), a 1st order µFPF and the new module with PbSe detector and a 3rd order µFPF.

First tests of a complete microspectrometer setup were conducted with a MEMS IR emitter (Intex MIRL 17-0900) and the conventional stepwise measurement method with a modulation frequency of 10 Hz. A 0.4 mm thick polystyrene foil served as a long term stable reference sample. It exhibits narrow band spectral features within the range of interest, which made it very easy to asses the spectral resolution of the setup. Figure 9 shows the measured spectrum with a new 3^{rd} order µFPF, an older version in the 1^{st} order as well as an FTIR measurement for comparison.

4. SUMMARY

A new µFPF for the measurement of hydrocarbon gases in the range $(3.1 \ldots 3.7)$ µm with a spectral resolution of $(20 \ldots 30)$ nm or even better has been presented. With a dualband configuration the parallel measurement of CO_2 in the range $(4.0 \ldots 4.6)$ µm is possible without compromising the overall performance of the filter.

The filters were combined with a room temperature lead selenide detector, which can potentially enable high scanning speeds. First experiments have prooved the increased spectral resolution under practical measurement conditions. Further tests with the focus on fast scanning methods and the signal-to-noise ratio are ongoing. Results will be subject of future papers.

The authors acknowledge the support by the Federal Ministry of Education and Research (Germany), contract number 13N12037.

REFERENCES

1. National Institute of Standards and Technology, "NIST Chemistry WebBook," (2013).
2. Kastner, J., "Aspects of process measurement in the natural gas industry," in [*VDI Fachkonferenz Prozess-analytische Messtechnik in der Chemieindustrie*], 97–118, VDI Wissensforum GmbH, Düsseldorf (2011).
3. Saptari, V. and Langridge, S., "A tunable filter optical system for on-line and real-time hydrocarbon gas composition analysis," in [*ISA 58th Analysis Division Symposium*], (2013).
4. Saptari, V., "Multiplex tunable filter spectrometer," (2010).
5. Neumann, N., Ebermann, M., Kurth, S., and Hiller, K., "Tunable infrared detector with integrated micromachined Fabry-Perot filter," *Journal of Micro/Nanolithography, MEMS and MOEMS* **7**(2), 021004 1–9 (2008).
6. Mannila, R., Tuohiniemi, M., Mäkynen, J., Näkki, I., and Antila, J., "Hydrocarbon gas detection with microelectromechanical Fabry-Perot interferometer," in [*Proc. SPIE 8726, Next-Generation Spectroscopic Technologies VI*], (2013).
7. Vaughan, J. M., [*The Fabry-Perot Interferometer: History, Theory, Practice and Applications*], Hilger, Bristol (1989).
8. Ebermann, M., Neumann, N., Hiller, K., Gittler, E., Meinig, M., and Kurth, S., "Widely tunable Fabry-Perot filter based MWIR and LWIR microspectrometers," in [*Proc. SPIE 8374, Next-Generation Spectroscopic Technologies V*], 83740X 1–9 (2012).
9. Schröter, J. R., Lehmann, S., Ebermann, M., and Neumann, N., "Wavelength stabilization of electrostatically actuated micromechanical infrared Fabry-Pérot filters," in [*Proc. SPIE 8868, Infrared Sensors, Devices, and Applications III*], 88680J 1–12 (2013).
10. Lehmann, S., Ebermann, M., and Neumann, N., "Charge control of electrostatically actuated micromachinal infrared Fabry-Pérot filters," in [*Proc. SPIE 8896, Electro-Optical and Infrared Systems: Technology and Applications X*], 889613 1–9 (2013).
11. Johnson, T. J., Simon, A., Weil, J. M., and Harris, G. W., "Applications of time-tesolved Step-Scan and Rapid-Scan FT-IR spectroscopy: Dynamics from ten seconds to ten nanoseconds," *Applied Spectroscopy* **47**(9), 1376–1381 (1993).
12. Hamamatsu Photonics K. K., Solid State Division, "Technical Infomation SD-12: Characteristics and use of infrared detectors," (2011).